Wavelet-based Impulse Reconstruction in UWB-Radar

Klaus Pourvoyeur[1], Andreas Stelzer[1], Gerald Ossberger[2], Thomas Buchegger[2], and Markus Pichler[2]

[1]Johannes Kepler University, Institute for Communications and Information Engineering, Altenberger Str. 69, A-4040 Linz, Austria

[2]Linz Center of Competence in Mechatronics, Altenberger Str. 69, A-4040 Linz, Austria

Abstract — **In this paper we present a technique for evaluating shape and position of an Ultra Wideband pulse in noisy data, based on the Continuous Wavelet Transformation. By using a complex extension for both, the signal and the mother wavelet, the received impulse can be completely characterized by only four parameters without the necessity of exact knowledge of the pulse shape. With this novel approach the impulse shape is characterized by the angle information of the complex wavelet transform. This allows e.g. to reduce the amount of data for further processing.**

I. Introduction

Ultra Wideband (UWB) signal transmission is a potentially promising technology that is characterized by a large fractional bandwidth, mostly based on very short pulses with a duration of approximately 0.5 to 2 ns each [5]. This technology can be used e.g. for radar, and especially for Ground Penetrating Radar (GPR), enabling high precision and penetration through the surface [6], [7].

The UWB-radar transmits an impulse, which is reflected by an object – usually called target for historic reasons – whose distance s can be evaluated if velocity and time-difference between transmission and reception of the pulse are known.

For the detection of the impulse covered by noise conventional correlation methods like the matched filter concept suffer one major drawback in analyzing the sampled signal: the requirement of the exact knowledge of the impulse shape. This information is not available in real UWB systems. The continuous wavelet transformation (CWT) can handle translated and dilated versions of a waveform, but the analysis wavelet has to be chosen properly to match the specific form of the searched impulse.

In this contribution we present a complex extension for the CWT giving this transformation the ability to deal with different forms of impulses, with a-priori knowledge of only the approximate pulse shape.

II. UWB System

A UWB impulse radar test setup was built to generate real radar reflection data. We used a pulse generator and a pulse forming network from Picosecond Pulse Labs, to generate a 100-ps pulse with an amplitude of –1.7 V and a pulse repetition rate (PRI) of 500 kHz.

The output of the pulse generating network was connected to a UWB transmitting antenna. The radiated pulse was reflected by a 600 mm × 450 mm copper plate and received by an antenna similar to the transmitting antenna. Sampling and displaying was done with a Tektronix 11801C sampling oscilloscope, which was triggered by the pulse generator. Wavelet-based impulse reconstruction was used to evaluate the exact position of the plate. Fig. 1 shows the implemented UWB-radar test setup.

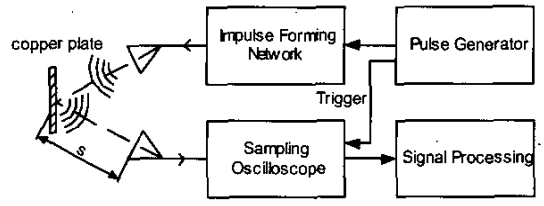

Fig. 1. UWB-radar test setup.

III. Complex Continuous Wavelet Transform

The CWT provides a method for the analysis of a signal $f(t)$ based on a single, possibly complex-valued, scaled, stretched and shifted mother wavelet ψ_p. At time b and scale a this transformation is defined as

$$W_f(a,b) = \int_{-\infty}^{\infty} f(t)\frac{1}{\sqrt{a}}\psi_p^*\left(\frac{t-b}{a}\right)\mathrm{d}t, \qquad (1)$$

where $\psi_p^*(\cdot)$ denotes the complex conjugate of $\psi_p(\cdot)$. The complex weights $W_f(a,b)$ can be interpreted in terms of magnitude and phase.

The generation of the mother wavelet starts with the complex Gaussian function

$$g(t) = C_p\, e^{-jt} e^{-t^2} \qquad (2)$$

centered around zero. The mother wavelet ψ_p is formed by taking the p-th derivative of the complex Gaussian function, and the coefficient C_p is chosen to satisfy the normalization condition

0-7803-7695-1/03/$17.00 © 2003 IEEE

$$\psi_p(t) = g^{(p)}(t) \quad \text{with} \quad \left\| g^{(p)} \right\|_2 = 1 \tag{3}$$

$$\|x\|_2 = \sqrt{\int_{-\infty}^{\infty} x(\tau) x^*(\tau) \mathrm{d}\tau} \,. \tag{4}$$

If p is even, the real part of ψ_p is an even function and the imaginary part is odd, and vice versa for an odd p; from this it directly follows that these two components of the wavelet are orthogonal to one another,

$$\int_{-\infty}^{\infty} \underbrace{\mathrm{Re}\{\psi_p(t)\}}_{\text{even(odd)}} \underbrace{\mathrm{Im}\{\psi_p(t)\}}_{\text{odd(even)}} \mathrm{d}t = 0 \,. \tag{5}$$

Fig. 2 shows the real and imaginary part of the mother wavelet ψ_p for $p = 2$. For further information concerning complex wavelets we refer to [2]-[4].

Instead of using the measured signal $f(t)$ directly for evaluation, the analytic signal $f^+(t)$

$$f^+(t) = f(t) + j\,\mathrm{H}\{f(t)\} \tag{6}$$

obtained from application of the Hilbert transform

$$\mathrm{H}\{f(t)\} = \frac{1}{\pi} \int_{-\infty}^{\infty} \frac{f(\tau)}{t-\tau} \mathrm{d}\tau \tag{7}$$

is taken. All spectral components of the original signal are shifted by $\pi/2$ rad. The signals $f(t)$ and $\mathrm{H}\{f(t)\}$ are frequently said to be in quadrature. In time domain, the signals $f(t)$ and $\mathrm{H}\{f(t)\}$ are orthogonal,

$$\int_{-\infty}^{\infty} f(t)\mathrm{H}\{f(t)\} \mathrm{d}t = 0 \,. \tag{8}$$

For the special case of even functions the Hilbert transform is odd and vice versa. For additional information we refer to [1] and [2]. Fig. 3 shows a measured UWB-radar signal and its Hilbert transform.

Since there is little difference in analysis results when using the analytic signal with a real-valued wavelet, or the real-valued signal with a complex wavelet only one case is visualized (Fig. 4 (a)). In both cases the magnitude of $W_f(a,b)$ shows some slight side maxima separated from the main peak.

Fig. 4 (b) shows the absolute value of the wavelet transform using the 2nd derivative of the complex Gaussian function as mother wavelet analyzing the analytic signal. For one single impulse the magnitude of the CWT shows almost no side maxima.

The results for real wavelets on the measured signal even if properly chosen show several major side maxima (Fig. 5 (c) and (d)). In case of heavy noise this drawback of the classic CWT makes it almost impossible to elicit several targets represented by multiple impulses.

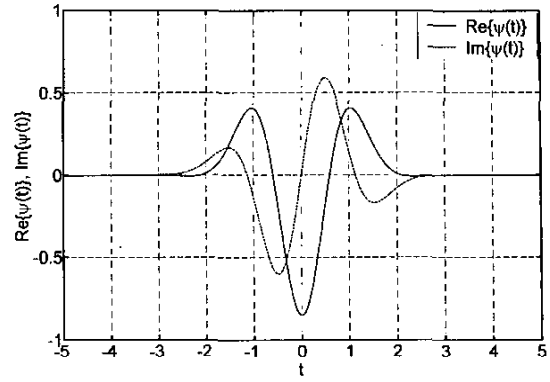

Fig. 2. Real and imaginary part of the complex mother wavelet for $p = 2$.

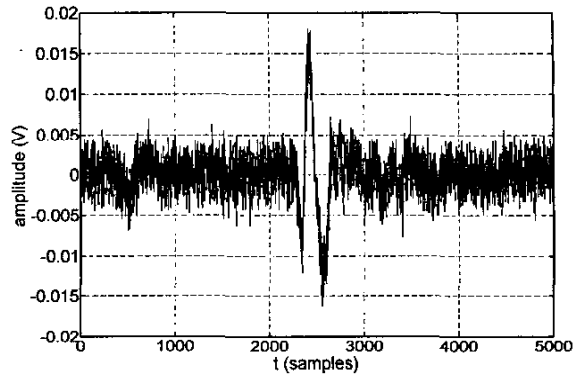

(a)

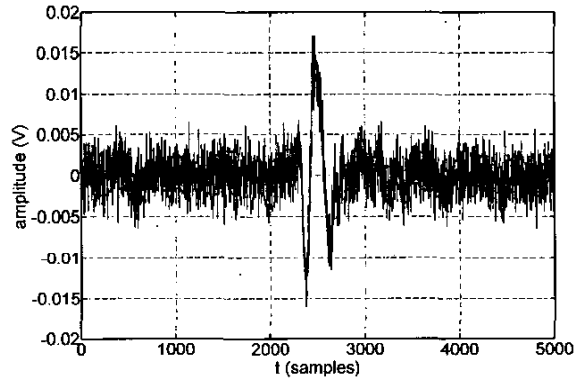

(b)

Fig. 3. (a) Measured UWB-radar signal and (b) its Hilbert transform.

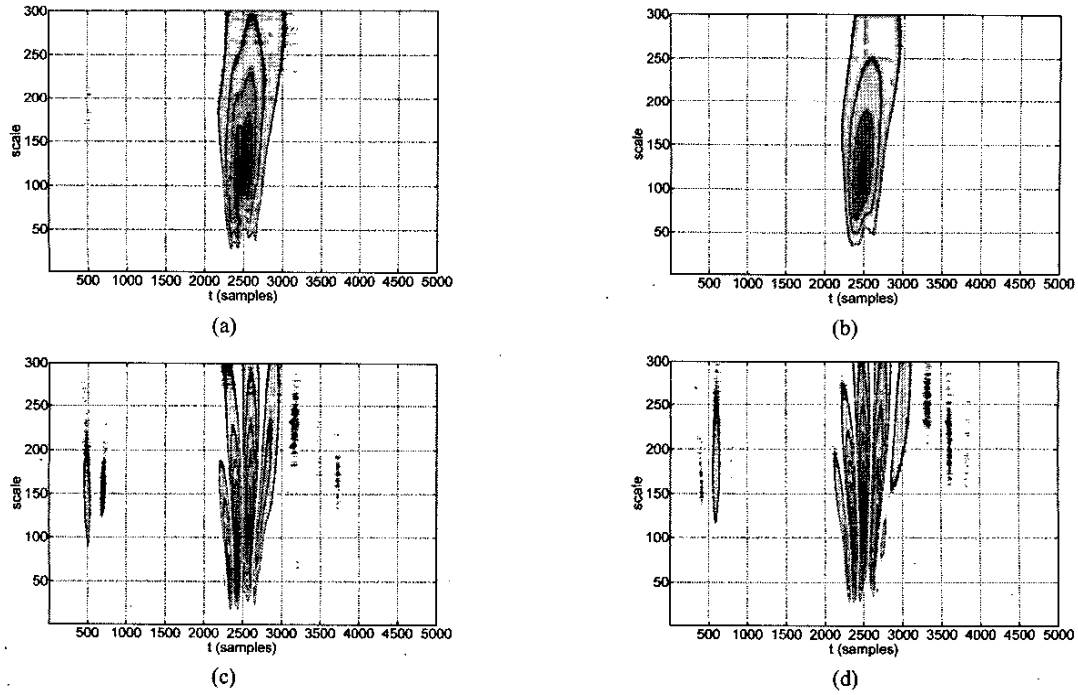

Fig. 4. Absolute value of the wavelet transform using the 2nd derivative of the complex Gaussian function as mother wavelet on (a) the measured and (b) the analytic signal as well as the magnitude using (c) the 2nd and (d) the 3rd derivation of the real Gaussian pulse as mother wavelet analyzing the real signal.

The angle information of $W_f(a,b)$ is visualized as grey-scale plot between $-\pi$ and π rad in Fig. 5, with phase jumps resulting from visualization effects.

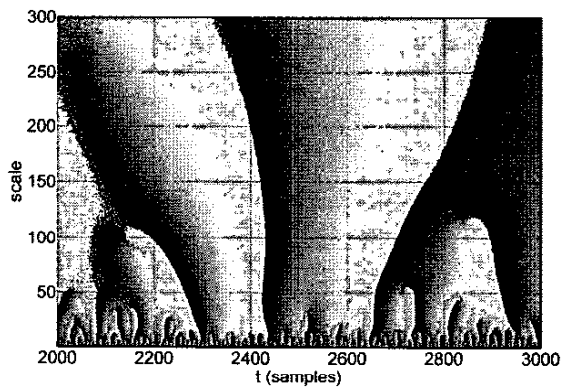

Fig. 5. Angle information of the complex CWT on the analytic signal using the 2nd derivation of the complex Gaussian function as mother wavelet.

IV. Impulse Reconstruction

For a better performance of this impulse reconstruction algorithm we propose at first to smooth the real and imaginary part of $W_f(a,b)$ separately by a filter based on a two-dimensional convolution with filter function Q

$$W_Q(a,b) = \int_{-\infty}^{\infty}\int_{-\infty}^{\infty} W_f(a',b')Q(a-a',b-b')\,da'\,db' . \quad (9)$$

Starting with the complex CWT of the analytic signal we search for the argument of the maximum absolute value of $W_f(a,b)$. This argument specifies both, the translation and dilatation, which characterize the received impulse

$$(a_m,b_m) = \arg\max_{(a,b)} \left| W_f(a,b) \right| . \quad (10)$$

Fig. 6 displays the relationship between the angle of the complex weight $W_f(a_m,b_m)$ (Fig. 5) and the impulse shape found by the complex CWT.

To acquire the impulse itself we evaluate the inverse wavelet transform for only one point in the scalogram given by a_m and b_m. $W_f(a_m,b_m)$ is the complex weight for the scaled, stretched and shifted mother wavelet.

$$f_{imp}(t) = \mathrm{Re}\left\{ W_f(a_m, b_m) \frac{1}{\sqrt{a_m}} \psi_p\left(\frac{t - b_m}{a_m} \right) \right\} \quad (11)$$

Fig. 7 shows the results of the impulse reconstruction of the measured UWB-radar-signal comparing real and complex wavelets.

V. Discussion

An impulse covered by noise is characterized by only four parameters: 1. translation b_m and 2. dilatation a_m of the mother wavelet as well as 3. the absolute value and 4. the angle of the complex weight $W_f(a_m,b_m)$. The value of b_m specifies the position of the searched impulse, a_m is a measure for its center frequency. The absolute value of the complex weight is a quantum for the impulse intensity, its angle classifies the shape of the impulse as shown in Fig. 6.

Another significant advantage of this complex expanded signal evaluation over conventional correlation concepts is its insensitivity to deviations of the noise-covered impulse from the expected pulse-shape. As Fig. 7 shows, the best match with the original impulse is achieved with the complex wavelet, whereas the even and odd wavelets show significant deviations in parts of the signal.

For a precise impulse analysis, especially for position detection, we propose to first reconstruct the impulse instead of taking one of the four parameters directly.

Another useful property of this complex extension to the CWT beside its independence to the impulse form is its resistance against heavy noise. A decreasing SNR has almost no influence on the position of the impulse characterized by the position of its maximum value, it varies only a few samples.

VI. Conclusion

The superiority of the proposed algorithm described in this paper over conventional evaluation is the characterization of a single impulse covered by noise by only four parameters without the necessity to properly select the mother wavelet. The major innovation is that the impulse shape is characterized by the angle information of the complex CWT. For one single impulse the magnitude of the CWT using a complex extension for both, the signal and the wavelets, shows almost no undesired side maxima.

Acknowledgement

The authors benefited from frequent discussions with E. Kolmhofer and C. Diskus of the Institute for Microelectronics, University of Linz.

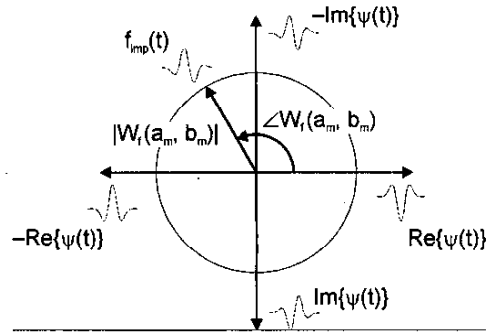

Fig. 6. Shape of the UWB impulse corresponding to the angle of the complex weight $W_f(a_m,b_m)$.

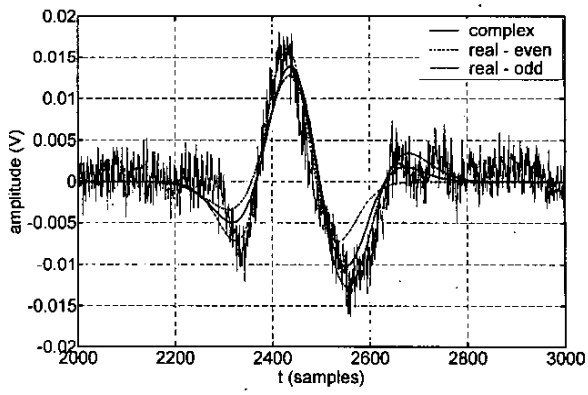

Fig. 7. Impulse reconstruction of a measured UWB-radar-signal using the 2nd (even) and 3rd (odd) derivative of the Gaussian pulse as well as the 2nd derivative of the complex Gaussian function as mother wavelet on the analytic signal.

References

[1] S. L. Hahn, *Hilbert Transforms in Signal Processing,* Norwood, MA: Artech House, 1996.

[2] A. D. Poularikas, *The Transforms and Application handbook,* Boca Raton, FL: CRC Press LLC, 2000.

[3] S. Mallat, *A Wavelet tour of signal processing,* Academic press, 1998.

[4] I. Daubechies, *Ten Lectures on Wavelets,* Philadelphia, PA: SIAM, 1992.

[5] C. L. Bennett and G. F. Ross, "Time-Domain Electromagnetics and Its Applications," *Proc. IEEE,* vol. 66, pp. 299-318, 1978.

[6] B. Scheers, Y. Plasman, M. Piette, M. Acheroy, and A. Vander Vorst "Laboratory UWB GPR system for landmine detection," in *Proc. 8th International Conference on Ground Penetrating Radar,* pp. 747-752, 2000.

[7] B. Sai and L. P. Ligthart, "Improved GPR data preprocessing for detection of various land mines," in *Proc. 8th International Conference on Ground Penetrating Radar,* pp. 80-84, 2000.